Agricultural Water Management 260: 107300 (2022)

Normalized pressure: a key variable to assess zebra mussel infestation in pressurized irrigation networks

Mario Morales-Hernández[1], Enrique Playán[2], Borja Latorre[2], Francisco Montoya[3], Cristina Madurga[4], Alejandro Sánchez de Rivera[4] and Nery Zapata[2]

Abstract

The impact of zebra mussel (*Dreissena polymorpha*) colonization on pressurized irrigation systems is becoming important in many areas of the world. If the infestation is not controlled, the conveyance capacity of the network reduces and mussels can completely block the system, preventing irrigation. A methodology to assess zebra mussel infestation in collective pressurized networks based on monitorization and hydraulic simulation is developed in this research. Normalized pressure, defined as the difference between simulated and measured pressure, is an indicator of the presence of zebra mussels (Morales-Hernández et al., 2018). When this variable is combined with the distributed discharge of the irrigation network, it is possible to use an optimization procedure to produce a roughness map of network pipelines. Roughness in excess of that characteristic of the pipeline material can be directly associated zebra mussel infestation. Different objective functions, optimization algorithms and strategies are proposed in this work, with the aim of attaining constant discharge-independent normalized pressure at each observation point in the network. Roughness values under different pipe conditions, reproducing levels of zebra mussel infestation, were experimentally obtained at a reference laboratory. The limitations and uncertainties of the proposed methodology are discussed. Normalized pressure was validated in an irrigation network belonging to a water users association, using continuous data recorded at different observation points during a complete irrigation campaign. The non-

[1] Fluid Mechanics Dept., Universidad de Zaragoza. María de Luna, 3, 50018, Zaragoza, Spain
[2] Dept. of Soil and Water, EEAD-CSIC. Avda Montañana 1005, 50059 Zaragoza, Spain
[3] CREA-UCLM. Centro Regional de Estudios del Agua. Carretera de Las Peñas, km 3,2 02071Albacete, Spain.
[4] CENTER. Central Laboratory for Irrigation Equipment and Materials Testing. Camino de la Vega s/n. San Fernando de Henares. 28830 Madrid, Spain.

invasive hydraulic method has been designed to identify infested areas in real time and to optimize the chemical treatments controlling mussel development

Keywords: Dreissena polymorpha, irrigation networks, hydraulic simulation, normalized pressure, optimization, pipe roughness.

1. Introduction

Zebra mussels (*Dreissena polymorpha*) are causing extensive damage to hydraulic infrastructure, as they reproduce inside water conduits and attach to many different types of surfaces. Severe problems have been reported in fluvial systems and lakes (Aldridge et al., 2004; Wimbush et al., 2009; Nakano and Strayer, 2014; Olson et al., 2018; Morales et al., 2019; Catita et al., 2020), but also in pressurized irrigation networks (Araujo et al., 2006; Morales-Hernández et al., 2018).

Zebra mussel has become an important restriction for the management of pressurized collective irrigation networks supplied from colonized reservoirs, rivers or canals. The enormous volume of infested water, the high reproductive rate, the adaptation capacity of the species and the cost efficiency required for agricultural production make it very difficult to eradicate the mussel in these water bodies. Therefore, control measures are required to reduce its impact.

The US Geological Survey set up a monitoring network to detect the presence of zebra mussel in many water bodies around the country. Benson et al. (2021) reported that piping irrigation systems downstream an infested water body are very likely candidates for infestation. In Canada, the Alberta Irrigation Districts (704 k ha of irrigated land) have recognized that the extensive irrigation network, particularly the underground pipeline network, could experience significant reductions in water conveyance capacity if invasive mussels colonize irrigation water supply reservoirs. The Government and the irrigation districts of the region are preventing the introduction of the species in irrigation water supply reservoirs, and recommending control and eradication measures if zebra mussel eventually infest irrigation water supply canals, pipelines, and on-farm irrigation systems (Paterson, 2018). In Spain, the Ebro, Jucar, Segura and Guadalquivir river basins authorities have reported several reservoirs colonized by zebra mussel supplying water to irrigation districts. Monitoring networks to detect and quantify infestation have been established. The Ebro river basin has the largest number of colonized reservoirs of the Spanish territory (CHE, 2018). Morales-Hernandez et al. (2018) reported that in Riegos del Alto Aragón project (RAA, 120 k ha of irrigated land in the Ebro river basin), reservoirs are colonized by zebra mussel. As a consequence, 66% of the irrigated area is infested. These authors documented the extent of the zebra mussel dispersion from the colonized reservoir to the piping irrigation systems and the control measures adopted by the irrigation districts to control the species.

The physical conditions of irrigation reservoirs are adequate for mussel reproduction and growing (Araujo, 2006). Colonized reservoirs act as permanent source of larvae for downstream water bodies and irrigation systems. Intensive zebra mussel invasion of irrigation pipes has been found to occur mainly during the juvenile stage of planktonic veligers (Zhang et al., 2017). Veligers first move freely in the water. At an age of 18-90 days, veligers adhere to hard substrates (Roberts, 1990) resulting in biofouling, pipe clogging and decreasing water transport efficiency. Pipe colonization is a gradual process that reduces the effective diameter of the pipe and increases its roughness. If the infestation is not controlled, the conveyance capacity of the network reduces and mussels can completely block the system, preventing irrigation. .

The two major problems of the recently modernized irrigation systems identified by the farmers in the RAA project are electricity cost and zebra mussel colonization (Morales-Hernández et al., 2018). A dense network of canals and small water derivations connect the natural water bodies and reservoirs with the irrigated areas of a large part of the Spanish irrigated land. This particularity has facilitated and accelerated dispersion of zebra mussels as compared with other countries (Araujo, 2006).

The effect of zebra mussel colonization of pipes can be compared to the accumulation of suspended particles on the inside wall of aged pipes. The roughness of the inner pipe wall affects the pressure drop of a fluid flowing through that pipe. This additional roughness can be hydraulically described as a constriction of the flow area and as an increase of the wall shear stress (Kandlikar et al., 2005).

Collective irrigation networks are more likely to be colonized than on-farm irrigation networks, since the former are closer to the infested water bodies. However, if the infestation of collective pipelines is not controlled, the on-farm network can be colonized too. The early detection of zebra mussel adults and shells in collective pressurized irrigation networks is a complex experimental problem. Most pipelines are buried in agricultural fields, so it is necessary to rely on indirect measurements of zebra mussel presence and on hydraulic simulations. Key elements of these networks include pipelines, hydrants (points of water delivery to farms), and often pumping stations (responding to water demand at the hydrants). Hydrants are usually accessible for hydraulic measurements. The combination of sensors and hydraulic simulation has been successfully applied in the past to other problems, such as monitoring water leaks (Pérez et al., 2011; Abdulshaheed et al., 2017) and pressurized network calibration (Walski 2000 and 2004; Kumar et al., 2010). This methodology was recently used to introduce the concept of normalized pressure in the context of zebra mussel infestation of collective irrigation networks (Morales-Hernández et al., 2018). Normalized pressure was defined as the difference between simulated and measured pressure at a certain point of a given irrigation network. The difference could be related to the presence of zebra mussels obstructing water flow. The method was validated by Morales-Hernández et al. (2018) using two different test cases: a discrete chemical treatment and the analysis of three years of telemetry pressure data in three remotely controlled hydrants.

In a collective irrigation network, a period without hydrant openings or closings is a stationary period. These periods minimize measurement uncertainties since changes in flow velocity and pressure are not expected. Hydraulic pipe simulators such as EPANET (Rossman, 2000) can obtain adequate results under these conditions, providing a complete characterization of the network (Morales-Hernández et al., 2018). However, errors resulting from incorrect network characterization (such as the length, diameter and roughness of each pipeline) are carried over thorough the numerical simulations. Such errors can prevent the extraction of adequate conclusions.

Uncertainties related with the network characterization and the hydraulic measurements require optimization methods to minimize errors in the estimation of parameters such as roughness. Two main optimization method families can be distinguished: derivative-free search algorithms (Mugunthan et al., 2005) and gradient-based methods (Chaparro et al., 2008). Although the latter set of methods could be more efficient for smooth function errors because they can obtain the optimal value, they require the gradient to perform the optimization, that is, the variation of the objective function with respect to the controlled variable. Obtaining the gradient can be complex when dealing with an external software. On the other hand, derivative-free algorithms are usually able to detect the optimal interval in the global solution space at the extra cost of large computational burden and low efficiency, since an extensive number of function evaluations is required. Some of the most popular optimization methods are included in NLopt (Johnson, 2017), a set of free/open-source libraries for nonlinear optimization. The optimization subroutines are implemented in different languages so they can be called from C, Fortran or Matlab, among others. The BOBYQA algorithm (Powell, 2009), with a classical least squares objective function, is an interesting optimization subroutine, since its supports local optimization subject to bounds on the variables.

Chemical treatments are the most effective control measures for agricultural irrigation networks (Waller and Fisher, 1998; Paterson, 20018; Morales-Hernández et al., 2018). Chemicals are required that are effective, fast and have minimum environmental impact and cost. The local conditions (water quality, quantity, irrigation network, environmental constrains and infestation level) should always be considered when selecting a chemical treatment. Early detection and location of colonized areas within the network will reduce the economic and environmental cost of the chemical treatment.

The aim of this research was to progress in the development of the normalized pressure method for the early detection and location of zebra mussel infestation in irrigation network pipelines. The following specific objectives were set:

1. To characterize and minimize experimental data error in water pressure measurement;
2. To explore different optimization methods to obtain roughness estimates at different observation points in a collective pressurized network;
3. To apply the normalized pressure method to a complete collective irrigation network, focusing on the spatial characterization of roughness; and
4. To estimate the infestation level by assigning the estimated roughness values to a proxy of infestation in experimental pipelines.

2. Materials and methods

2.1. Normalized pressure and network discharge

The hydraulic simulation required to determine normalized pressure should consider the condition of the network at the measurement time and location. Since network hydraulics periodically change with the opening and closing of hydrant valves, normalized pressure is only meaningful when stationary periods of network operation are considered. Irrigation telemetry and remote control (TM/RC) systems are frequently installed in the modern irrigation networks of Spain (Playán et al., 2018). Such systems can produce the data required to identify stationary periods in a time series of network operation data.

Pressure can be simulated throughout the pipelines of collective irrigation networks using a hydraulic piping network software such as EPANET (Rossman, 2000). An adequate characterization of pipeline diameters, lengths and roughness, as well as the elevation of nodal points is required for adequate simulation. Pressure measurements can be experimentally obtained using pressure transducers installed at specific network points, usually the network hydrants.

Morales-Hernández et al. (2018) used normalized pressure to identify the presence of zebra mussels (adult or shells). In a pipe, high and positive values of normalized pressure indicate infestation, while values close to zero suggest that the pipe is essentially clean of mussels. This rule is based on the concept of head loss in hydraulic modeling. When simulated pressure exceeds measured pressure, head losses are underestimated in the simulation.

Total pressure losses h_f can be characterized by the friction factor f (dimensionless) using the Darcy–Weisbach equation (1), where L is the pipeline length, D the diameter, v the flow velocity and g the gravitational acceleration:

$$h_f = f \times \frac{L}{D} \times \frac{v^2}{2 \times g} \tag{1}$$

The empirical Colebrook-White equation expresses the Darcy friction factor f as a function of Reynolds number (Re), the pipe hydraulic diameter (D_h) and the absolute roughness coefficient (ε_c):

$$\frac{1}{\sqrt{f}} = -2log\left(\frac{\varepsilon_c}{3.7D_h} + \frac{2.54}{Re\sqrt{f}}\right) \tag{2}$$

Therefore, it is feasible to predict in a qualitative way the behavior of normalized pressure (P_N) in a pipeline with respect to discharge in the case of choosing the correct absolute roughness coefficient (ε_c), an overestimated (ε_o) or an underestimated (ε_u) value. The effect on normalized pressure of the selected coefficients as a function of discharge is presented in Figure 1.

As observed, in the case of an adequate estimation of the absolute roughness coefficient, P_N should remain invariant: the difference between simulated and measured pressure is discharge-independent. When an overestimated absolute roughness coefficient is used, P_N will decrease its value as discharge increases. Conversely, P_N will increase with discharge when an underestimated value of the absolute roughness coefficient is used. It is worth remarking that the influence of the roughness factor is negligible for low discharge values. Indeed, the three normalized pressure curves tend to the same value (δ) for $Q = 0$, i.e., when the system becomes hydrostatic.

This theoretical analysis referred to a pipeline can be extrapolated to a network composed by several pipelines and a number of pressure observation points. Since normalized pressure is only valid for networks in which the demand at all hydrants is known, the total discharge delivery (Q_D) understood as the sum of all hydrant demands, can be considered as a representative variable of the hydraulic network.

2.2. La Violada Network, Almudévar Water Users Association

The *Almudévar* Water Users Association (AL-WUA), with a total extension of 3,744 ha, is located in the central Ebro River Valley (Figure 2a) and in the northwest part of the *Riegos del Alto Aragón* project (Figure 2b). This WUA was modernized from surface to pressurized irrigation (typically sprinkler irrigation solid-sets) between 2008 and 2010. AL-WUA has five independent irrigation networks, each one including a pumping station, a reservoir and a TM/RC system with the capacity to issue hydrant valves and farm sector valves opening and closing orders and registering hydrant discharge. One of the irrigation networks, called "La *Violada",* covers an irrigated area of 1,400 ha (Figure 2c). This network was used to develop and validate the method presented in this paper. The information provided by the TM/RC database was used to identify stationary periods of network operation.

Ten pressure transducers were installed at hydrants H226, H234, H241, H243, H249, H256, H260, H261, H264 and H275 (Figure 2c). Transducers were strategically located following the identification by the AL-WUA management of network branches suffering from intense zebra mussel infestation. Pressure monitoring covered an irrigation campaign (from June to mid-October 2017).

Two types of hydrants can be distinguished in the network: transport and service hydrants. A transport hydrant not only gives service to one or several farms, but its upstream and downstream pipelines convey a large amount of water to supply distant irrigated areas. Hydrants H226, H256 or H261 exemplify transport hydrants. Hydrants located near the end of network branches carry a low flow discharge though their upstream and downstream pipelines (if any). H241, H249 or H275 are examples of service hydrants.

2.3. Minimizing data uncertainties

The quality of measured and simulated pressure data requires some discussion. There are different sources of uncertainty that need to be controlled to obtain adequate results from the proposed method.

A non-infested network should have a constant, zero value of normalized pressure. Any non-zero value of δ (Figure 1) implies an error in pressure measurement and/or a deficient hydraulic characterization of the network. The pressure transducers used in this research (model Dickson PR325) had a manufacturer accuracy of 1%. All sensors were verified at the laboratory before their installation in the field. A high-precision pressure measurement instrument (model WIKA PCH6400) was used for this verification. Devices with measurement errors exceeding the manufacturer specifications were rejected. Devices showing small deviations were assigned an *ad-hoc* calibration curve.

Pressure transducers were installed at the hydrant points (Figure 2c), at certain elevation from the underground pipeline network. The installation height of each pressure transducer was considered when comparing measured and simulated pressure at each observation point. Pressure transducers were equipped with a data logger programed to record pressure every minute. Data were periodically downloaded to a database.

Network characterization can also be a relevant source of error when assessing normalized pressure. Information about pipeline length, diameter and roughness was obtained from the construction project report. An absolute roughness coefficient of 0.01 mm was initially used in all pipelines, regardless of its material, diameter and installation. The location and elevation of all hydrants was corrected from the original project using altimetry data obtained with a high precision GPS receiver (model GS15 receiver Leyca Geosystems AG, Heerbrugg, Switzerland). GPS measurements were corrected in real time (RTK) using the permanent network of active geodesy of the

Aragón region of Spain, ensuring elevation errors lower than 0.02 m (Morales-Hernández et al., 2018).

The information about the discharge demand of each hydrant was not always complete at the TM/RC system. In those cases, the nominal hydrant discharge (obtained from the construction project report) was considered.

A pumping station is used to pressurize La *Violada* irrigation network. Variable frequency drives installed in the three pumps adjust flow and pressure to the actual water demand. These adjustments produce pressure oscillations that propagate through the network. A pressure transducer, installed just downstream of the pumping station, provide measurements every minute that are logged by the TM/RC SCADA. Pressure at this location was used as inflow boundary condition for the hydraulic simulation of the network.

The data series was filtered using a minimum stationary period duration of 10 minutes. In Morales-Hernández et al. (2018), a stationary period of 20 minutes was selected as a balance between computing time and accuracy. However, the choice of 10 minutes was more convenient in this work to provide a larger number of periods for the analysis of normalized pressure as well as to increase accuracy, leaving aside the computational burden.

The TM/RC database provided the hydrant configuration at the stationary periods and the pressure transducers installed at the network hydrants supplied pressure observations. These data should be synchronized and validated for simulation purposes. In order to select adequate stationary periods, the quality of pressure measurements at the pumping station was assessed. Three accuracy levels U1, U2 and U3 were defined according to their standard deviation σ_P (kPa) as reported in Equation (3):

$$U(\sigma_P) = \begin{cases} U3 & \sigma_P \leq 2 \\ U2 & 2 < \sigma_P \leq 5 \\ U1 & \sigma_P \geq 5 \end{cases} \quad (3)$$

Quality assessment was also applied to data measured at the hydrants using the pressure transducers. Given the frequency of pressure transducer data recording, a minimum of 10 pressure measurements were acquired at each stationary period. Since normalized pressure is determined using a unique pressure observation, an arithmetic mean was computed.

Finally, the computed normalized pressure for each hydrant and stationary period was screened to eliminate outliers. Figure 3a shows a conceptual plot of normalized pressure (P_N) at hydrant *i* against the network discharge delivery, Q_D. To identify outliers, Q_D was discretized in ranges and the mean normalized pressure was computed for each range. Any data point exceeding plus/minus two standard deviations was considered as an outlier. In this work, the discharge discretization interval was 200 l s^{-1}. Figure 3b presents the mean (continuous line) and the range of P_N (discontinuous line), as well as the outliers (cross symbols) for each discretized value of Q_D in the analyzed hydrant.

2.4. Optimization

Normalized pressure was computed for each stationary period at each monitored hydrant. The following step in data analysis was to determine optimum values of roughness of the simulated pipes that make normalized pressure constant for different values of Q_D. Optimization procedures were thus applied to obtain estimates of absolute roughness values for each pipe and each stationary period. Note that there is a direct relationship between monitored hydrants and estimated roughness values in this framework: pipes serving a large number of monitored hydrants will achieve more reliable roughness estimates than pipes serving few monitored hydrants - such as the north part of the piping network in Figure 2c. The determination of the optimum number of monitored locations given a certain network topology is an important issue, but it is out of the scope of this research work.

The nature of this optimization is complex since iterations are required over the roughness coefficient of several pipelines (multi-dimensional), satisfying the value of normalized pressure P_N at different hydrants (multi-objective) and for different total discharge deliveries Q_D (multi-scenario). The following constraints were imposed to the optimization problem and its solution: 1) the initial configuration of the network was defined by a constant roughness value of 0.01 mm for all pipelines; 2) a discharge-constant P_N is sought at each measured hydrant; 3) the range of the absolute roughness is 0.001 – 100 mm; 4) The derivative-free optimization algorithm BOBYQA (Powell, 2009) was used.

Different objective functions and topology strategies were analyzed in this research.

2.2.1. Objective functions

In optimization problems, the definition of an adequate objective function is the key to quick convergence to an appropriate solution. The general multi-objective optimization problem can be formulated via the minimization of the sum of different functions $f_i = f_i(P_{N_i})$ with different weights ω_i as follows:

$$\min \sum_i^N f_i^2 \omega_i \quad (4)$$

where i = 1…N, being N the number of measured hydrants. In this work, homogeneous weights ω_i = 1/N were adopted. As previously discussed, an intercept in the discharge - normalized pressure curve may exist due to experimental errors and assumptions (Figure 1). This intercept (δ_i) can be different for each measured hydrant i. Three different types of functions f_i were considered in this work, leading to three different objective functions.

Quasi-hydrostatic pressure

This method consists in computing the intercept δ_i as the average of P_{N_i} when Q_D is low (less than 50 l s^{-1}). This corresponds to a quasi-hydrostatic network status. Once δ_i is determined by an arithmetic mean, the function f_i is defined as follows:

$$f_i = P_N - \delta_i \quad (5)$$

Quadratic regression

The computation of the intercept δ_i in this method is based on fitting a quadratic regression without the linear term. The independent variable is Q_D, while the dependent variable is normalized pressure at hydrant *i* (P_{N_i}):

$$P_{Ni}(Q_D) = a_i Q_D^2 + \delta_i \quad (6)$$

The function f_i is built using Eq. (5) as in the quasi-hydrostatic case.

Null slope

The function f_i corresponds to the slope of normalized pressure with respect to network discharge. It is computed as follows:

$$f_i = \frac{\sum_{j=1}^{M} (Q_D^j - \overline{Q_D})(P_{Ni}^{\,j} - \overline{P_{Ni}})}{\sum_{j=1}^{M} (Q_D^j - \overline{Q_D})^2} \tag{7}$$

where M is the number of total steady configurations of the network to be analyzed and $\overline{Q_D}$ and $\overline{P_{Ni}}$ are the mean discharges and normalized pressures, respectively.

2.2.2. Network topology

The number of dimensions or parameters to be optimized is a key factor to the optimization problem. It governs not only the number of iterations of the optimization procedure (and consequently the computational time) but also the accuracy and unicity of the results. Making the number of dimensions equal to the number of pipelines in the network would be the best option, but the computational time would be unaffordable (La *Violada* network has 146 different pipes). In order to determine the number of dimensions, it is important to match the density of input data and results, and to use reasonable computation times.

Three levels of accuracy were proposed in this work by establishing zones grouping a number of pipelines. The network was divided in different zones whose pipelines will have the same absolute roughness coefficient. Figure 4 shows the network zones corresponding to the three optimization scenarios used in this research: three zones (Figure 4a), five zones (Figure 4b) and eleven zones (Figure 4c). Two zones remain the same in all three scenarios: zone 1 and zone 2. Zone 1 corresponds to the north side of the network, while zone 2 corresponds to the pipelines located near the reservoir and the pumping station. Zone 1 (red pipes in Figures 4a, 4b and 4c) was kept invariable because no pressure measurements were available in this network area and optimization could not be performed. The south area of the network (green pipes in Figure 4a) has the largest number of pressure measurements and was discretized in one, three and nine zones in the three optimization scenarios, respectively.

A sensitivity analysis was performed for the first optimization scenario (three zones, Figure 4a) to assess the influence of each zone on the results and the uncertainty and/or robustness of the solution. The baseline roughness (extracted from a previous optimization), lower limit, upper limit and size step values used in each zone are presented in Table 1.

2.5 From pipe absolute roughness to level of infestation

Experimental measurements of head losses were performed at a certified laboratory (Central Laboratory for Irrigation Equipment and Materials Testing, UNE-EN ISO/IEC 17. 025) for a pipe under different levels of obstacles to flow in its cross-sectional area. Obstacles were used as a proxy of the zebra mussel colonies established in a similar pipeline.

A PVC pipe of DN200 and 16 atmospheres (inner diameter of 170.4 mm) was used in the experiment. This diameter was adequate for laboratory measurements, and is within the small range of diameters used in pressurized irrigation networks. The laboratory can analyze head losses in pipe diameters DN200, DN250 and DN300. The measurement accuracy of pressure readings is 0.25%. The length of the analyzed pipe was 1.1 m, adequate for the laboratory monitoring equipment. To simulate zebra mussel effects on pipeline head losses, screws were inserted at different distances and to different depths (distance between screws of the same circular crown, ∂_{XD}, distance between circular crowns, ∂_{XL}, Figure 5a, and depths, ∂_{XH}, Figure 5b).

Figures 5a and 5b present the longitudinal and cross-sectional profiles of the experimental pipe. The values of the parameters defining the experimental conditions presented in Figure 5 are summarized in Table 2. Two spacings between screws (29.9 mm x 52. 4 mm and 59.8 mm x 104.8 mm, ∂_{XD} x ∂_{XL}, respectively) and four screw depths inside the pipes (∂_{XH} = 0, 20, 30 and 40 mm) were tested. In general, for each pipe configuration five discharges were evaluated (Table 2). Head losses were obtained for each condition. The Darcy–Weisbach equation (Eq. 1) and Colebrook implicit equation (Eq. 2) were used to determine absolute roughness.

3. Results

The proposed methodology was applied to La *Violada* network during the 2017 irrigation season. The AL-WUA TM/RC database provided 13,499 irrigation records from February 23 to December 30. Pressure transducers were installed at the hydrant points during the last week of May and were removed at the end of November. Pumping pressure data were available throughout the irrigation season.

The location and elevation of the 105 hydrants were measured, and the built project data was updated accordingly. The network length totalized 31,655 m, organized in 147 pipe sections with diameters ranging from 144 mm to 1,176 mm and with lengths ranging from 5 m to 1,120 m.

3.1 Data filtering

Data from June 1st to November 30th were processed. During this time, 3,875 stationary periods larger than 10 minutes were identified in the TM/RC database. Regarding the stability of pressure at the pumping station, 305 periods were classified as U1, 268 as U2 and 3,302 as U3 (85% of total). The most exigent accuracy level, U3, was selected because it provided an adequate accuracy and did not drastically reduce the number of stationary periods.

The total number of pressure measurements at each hydrant ranged from 200,943 at H249 to 219,682 at H261. Particularly, among all the stationary periods, the available measured data ranged from 89% for H249 to 100% for H226. The screening of normalized pressure data permitted to eliminate outliers at each hydrant. The number of outliers ranged from 2% at hydrant H256 to 5% at hydrant H241, with a mean of 3% among all hydrants. Note that this process makes that some stationary periods do not have pressure information at all hydrants at all time steps. However, only 1% of the stationary cases were finally discarded as they had less than 3 valid hydrant normalized pressure values. As a result, a total number of 3,269 stationary cases were used in this study.

3.2 Optimization

The proposed optimization methods, quasi-hydrostatic, quadratic-regression and null-slope, were applied to the three scenarios (3, 5 and 11 zones). Figure 6 presents the standard deviation of normalized pressure for the nine combinations and for the original (non-optimized) situation, i.e., with a constant roughness value of 0.01 mm for all pipes. In general, the largest variability corresponds to the most distant hydrant and the lowest to the closest hydrant to the network inlet. The improvement of all optimizations respect to the original situation is important at H241 (reduction form 18 kPa to 10 kPa) and H243 (reduction from 16 kPa to 8 kPa), non-relevant at H249 (Figure 6) and average at the rest of hydrants. Based on the standard deviation analysis, the quadratic regression optimization method was the most efficient in 6 out of the 10 hydrants - H234, H260, H264 and H275 applied to the 11-zone scenario and H226 and H241 for the 3-zone scenario. Conversely, the null slope method obtained the lowest standard deviation in H243 and H261 for the 3-zone configuration and in H249 for the 11-zone configuration. The quasi-hydrostatic method was preferred for hydrant H256. Note that the differences between the methods were usually in the order of 0.1 kPa in the standard deviation. Consequently, the different combinations of optimization method and zoning scenario had small implications on the standard deviation of normalized pressure. Only at H249 the 11-zones scenario showed lower standard deviation of P_N than the other two scenarios, with no differences between optimization methods. The standard deviation achieved after optimization was lower or equal to 10 kPa for all measurement hydrants.

The values of the intercept at the different hydrants, δ_i, for both quasi-hydrostatic and quadratic regression optimization methods (see equations (5) and (6) respectively) are displayed in Table 3. Values ranged from 8.4 kPa at hydrant H275 for the quadratic regression method to 51.8 kPa at hydrant H249 for both optimization methods. The difference between the intercepts (in absolute value) computed by one or the other method is at most 1.5 kPa.

Figure 7 illustrates the comparison between the original values of normalized pressure and the optimized P_N obtained with the best combination of optimization method and zoning scenario for four hydrants. The selected hydrants are: H226, the closest to the pumping station (Figure 7a); H243, with one of the largest dispersions of normalized pressure (standard deviation of 16 kPa, Figure 7b); H249, with the largest variability between optimization methods and no relevant improvements respect to the non-optimized situation (Figure 7c); and H256, with one of the lowest dispersions of P_N (Figure 7d). Hydrants with high dispersion on the original data maintain relevant dispersion after the optimization process (H243, Fig 7b). However, the standard deviation was reduced to half of the original value.

The optimization process provides the values of absolute roughness for each zone and optimization method (Figure 8). For example, for the 3-zone scenario (Figure 8a) the values of roughness strongly depend on the optimization method for zone 1 (values from 0.02 mm for the quadratic regression to 0.70 mm for quasi-hydrostatic), but show small differences for zones 2 and 3. This is particularly true for the quasi-hydrostatic and quadratic-regression methods, which provide excellent agreement for zones 2 (25 mm) and 3 (0.30 mm). The dependence on the optimization method for zone 1 relies on the lack of measurement points in this zone.

The maps of the absolute roughness of the pipes for the 3-zone (Figure 9a), 5-zone (Figure 9b) and 11-zone (Figure 9c) scenarios for the quasi-hydrostatic optimization method provide the estimated spatial distribution of the roughness coefficient. In a qualitative basis, the highest the roughness, the highest the zebra mussel colonization of the pipeline.

Zones 1 and 2 account for the same set of pipelines in the three sectoring scenarios (Figure 4). However, the optimized roughness values changed with the zoning scenario for zone 1 and remained almost constant for zone 2. Zone 1 presented lower roughness in the 3-zone scenario (0.02 to 0.70 mm, Figure 8a) than for the other scenarios: 5-zones (1.1 mm to 11mm, Figure 8b) and 11-zones (0.50 mm to 50 mm, Figure 8c). Zone 1 had no measurement devices, so roughness changes in this zone will not affect measurements. Only pipes with upstream/downstream pressure measurements can be optimized, since changes in their roughness will affect these measures.

Zone 2 corresponds to the network inlet. This is the shortest zone, with the largest pipeline diameters and only has one measurement point, located at its downstream end (H226). This zone has the largest roughness coefficient values for any of the studied configurations (Figure 8). Roughness values ranging between 25 and 30 mm are quite similar among optimization methods and zoning scenarios. The average normalized pressure of its measurement point was the lowest of all monitored points (9.9 kPa, Figure 7a) although the pipeline diameter is the largest (1.176 mm). The same level of zebra mussel infestation will provide smaller normalized pressures in large pipelines than in small pipelines. This can explain why the lowest normalized pressure resulted in the highest estimated roughness coefficient. Zone 2 was the most affected by zebra mussel colonization in all the analyzed conditions.

The southern part of the network has nine measurement points and was divided in 1, 3 or 9 zones. Zone 3 was quite similar for the 5-zone and 11-zone scenarios, and attained similar roughness in both scenarios. Roughness variability in this zone, from 0.02 to 0.30 mm, depends on the optimization method. Zone 4 of the 5-zone scenario, which was divided in zones 4, 5 and 6 in the 11-zone scenario, resulted in moderate roughness values (lower than 1 mm). Zone 8 of the 11-zone scenario is an end of network branch (Figure 4c) that delivers water to four hydrants and includes measurement point H249.

This zone has the lowest value of optimized roughness (0.001 mm, Figure 8c and 9c) indicating that zebra mussel infestation is low. The measurement point of this zone, H249, showed the largest values of intercept in the normalized pressure (51.8 kPa, Figure 7c) and had one of the smallest pipeline diameters, 181 mm. The large value of the intercept introduced uncertainty that could explain the low value of roughness coefficient. In addition, the small pipe diameter could explain why the highest normalized pressure provided the lowest value of roughness. However, the optimization process is a mathematical instrument to adjust data, which does not necessarily provide unique solutions.

3.3 Sensitivity analysis

To characterize the robustness of the optimization method and to justify the variability of the results for zone 1, a sensitivity analysis was performed for each of the zones for the quasi-hydrostatic method applied to the 3-zones scenario. The error, E, was computed following equation 8 and the sensitivity, φ, equation 9.

$$E = \frac{1}{NM}\sum_{i=1}^{N}\sum_{j=1}^{M}(P_{N_i} - \delta_i)_j \tag{8}$$

$$\varphi = \frac{\dfrac{E_{i+1} - E_i}{\frac{1}{2}(E_{i+1} + E_i)}}{\dfrac{\varepsilon_{i+1} - \varepsilon_i}{\frac{1}{2}(\varepsilon_{i+1} + \varepsilon_i)}} \tag{9}$$

where φ is the sensitivity, ε is the absolute roughness value, E is the error, M is the number of total steady configurations of the network and N the number of measurement points.

Figure 10 shows a scatter plot between values of roughness for each of the three zones (zone 1, zone 2 and zone 3, Figure10a, 10b and 10c, respectively) *versus* sensitivity (right axis) and error (left axis).

Zone 1 has a sensitivity equal to zero (Figure 10a), corroborating that zone 1 has no influence on the results. The error remains constant independently of the roughness value. The absence of pressure measurements inside the zone to adjust roughness values results in any value providing similar results. In order to provide sensitivity to this area, observation points should be added.

The sensitivity of zone 2 (Figure 10b) is lower than that of zone 3 (Figure 10c) (note the x-axis scale). A small change in the roughness coefficient of zone 2 has much less influence on the results than the same change in zone 3. In both areas sensitivity increases as we move away from the optimal solution (minimum error), but at different rates. Again, the larger number of measurement points in zone 3 (9 points) compared with those of zone 2 (on point) can explain the different sensitivity.

To assess the combined effect of the selected values between zones 2 and 3, a combined error analysis is presented in Figure 11. There is a wide strip of values in which the result of optimization becomes very similar, showing a similar error. Values of roughness between 16 to 34 mm for zone 2 and between 0.30 to 0.60 mm for zone 3 provide similar error values. A zoom in this strip of error values is presented in Figure 11b. The error scale ranges from 35 to 80 at Figure 11a and from 33.5 to 36 at Figure 11b. The sensitivity analysis of the optimization algorithm led to the global minimum. Consequently, the optimization method provided robust and consistent solutions.

Table 4 shows the results of computational time and number of iterations for each configuration. As the number of dimensions increased, the calculation time and the number of iterations required for convergence increased. However, there were no notable differences between optimization methods considering the same number of discretization zones. The computing time of the proposed algorithm for zebra mussel infestation assessment is affordable and the number of observations and zones can be increased without compromising its practical application.

3.4. From absolute roughness to zebra mussel infestation level

The total number of experimental measurements of head losses at the laboratory was 35. The different screw configurations inside the pipe were translated to occupied cross-sectional area, in percentage, considering the diameter of the screw, the distance between them and the depth into the pipe. The experiment performed with the maximum number of screws inserted at its maximum depth occupied 29.5% of the total pipe cross-sectional area and was considered as representative of an extremely-high colonization. The infestation levels proposed in this study were based on the cross-sectional area occupied by the screws: Extremely-high (> 25%), Very-high (from 20 to 25%), High (from 15 to 20%), Medium (from 10 to 15%), Medium-low (from 5 to 10%) and Low (from 0 to 5%).

Figure 12a presents the roughness coefficient experimentally obtained as a function of the cross-sectional area occupied by the screws, in %. The ranges of the infestation levels are also presented in the upper part of the Figure. Error bars represent the experimental variability of absolute roughness for the different values of discharge measured at each screw configuration (Table 2). In general, the variability of the roughness coefficient increased with the infestation level. For the same infestation level, the lower the discharge the larger the roughness coefficient.

The measurement performed with no screws resulted in low roughness values, ranging from 0.0013 to 0.002 mm, for the lowest and the highest discharge, respectively, with an average of 0.0016 mm. This average value is in the range proposed by manufacturers for PVC or other plastic pipes (0.0015 to 0.007 mm) and will be considered as the upper roughness limit for infestation-free pipes.

As the area occupied by screws grows, absolute roughness increases, reaching extremely high values (averaging 118.6 mm for the most occupied section area). A second grade polynomic equation was adjusted to fit the average values of absolute roughness as the useful section decreases (Figure 12a). The model is representative of the analyzed pipe (DN200 and D_{inner}= 170.4 mm). Its applicability to other diameters has not been tested. La *Violada* network has 32% of its pipes similar in diameter to the one used in this experiment. Around 65% of the pipes are smaller in diameter than DN300 mm, and only 2% of the pipes have diameters exceeding 1000 mm.

Several authors have indicated that with decreasing diameters, the relative importance of pipe surface roughness increases (Kandlikar et al., 2005; Taylor et al., 2006). Experiments with other diameters would be required to extend the obtained results to the rest of pipe sections in the network. The laboratory cannot evaluate the largest diameters present in the experimental network.

In the Moody diagram (Moody, 1944), the graphic form of the Colebrook´s equation, the friction factor increases with Reynolds number and asymptotically reaches a constant value at high Reynolds numbers. This relationship changes with the relative roughness. The values of relative roughness (ε/D) presented in this diagram ranged from 0 to 0.05.

Figure 12b presents an extension of the Moody diagram for a larger range of relative roughness, from 9.6E-06 to 0.6962, as measured at the laboratory. The laminar to turbulent transition occurs at lower Reynolds numbers as the relative roughness increases (Figure 12b).

As an exploratory exercise, the values of absolute roughness obtained for each zone with the proposed method (Figure 9), were transformed to infestation level following the adjusted model presented in Figure 12a. For the 3-zone and 5-zone scenarios, 94.5% of the total pipes have a low infestation level and the other 5.5% have a moderate-low infestation level. The 11-zone scenario showed different percentage of the infestation levels, with 2.8% of infestation-free pipes, 80.9% of low infected pipes and 16.3% of moderate-low infected pipes. Regarding the validity of the relationship between absolute roughness and infestation level, pipes with the largest diameter of the network (3 pipes of 1176 mm) were classified as moderate-low infected in the three scenarios, the largest infestation level of the network classification. This level of infestation of the large pipes should be carefully considered because of the previously discussed upscaling problems.

4. Discussion

Zebra mussel has a strong capacity to block large pipes and to colonize pressurized collective irrigation networks. The normalized pressure method has been applied in this study to determine the infestation level of zebra mussels in network pipes. The quality of measured and simulated pressure data is critical to the applicability of the P_N method. De Schaetzen et al. (2000) and Kumar et al. (2010) reported that measurement points should be selected as the most sensitive to changes in pipe roughness parameters. In this work, the measurement points were those identified by the district manager as the most problematic for zebra mussel. Consequently, these were the most likely to change the roughness of the underlying pipes. Walski (2000) indicated that data quality is an important and commonly ignored issue during calibration. Appropriate data are collected when there is sufficient head loss (larger than the measurement error) to draw valid conclusions. The uncertainty of data measurements at specific nodes and at the network inlet can be minimized by ensuring a low standard deviation of the measurements during the stationary periods.

Bezerra et al (2017), working on roughness calibration of piping networks with hydraulic simulation modeling, indicated that an adequate layout of the nodes with known pressures was more important than a large number of pressure measurements. To follow this recommendation, the location and elevation of all hydrants from the original project was revised using altimetry data obtained with a high precision GPS receiver. Even then, an important uncertainty in irrigation network hydraulic characteristics was identified in variable δ of the normalized pressure method. The method keeps this variable constant, excluding this uncertainty from the determination of P_N.

The selected approach for comparing observed and simulated nodal pressure and for adjusting the friction coefficients of pipes to obtain an acceptable tolerance of error resulted adequate to determine the infestation level of zebra mussel in pipes. Most efforts towards model calibration have been undertaken by adjusting roughness coefficients alone; the reduction in pipe diameter has often been neglected (Boxall et al., 2004). This simplification has often been found to adequately predict pressure distribution and flow balance at each node in the system (Walski, 2004); however, the representation of the flow paths and velocity distribution may not be well predicted. Many water quality problems including disinfectant decay (Hallam et al. 2002; Clark and Haught, 2005), disinfection by-product formation, and taste and odor problems have been associated with the residence time of water in distribution systems (Christensen and Barfuss, 2009). This approach is also necessary when applied at mini and micro-pipes where the relative size of the roughness with respect to the pipe diameter grows dramatically (Taylor et al. 2006). In this study, neither the velocity nor the micro pipes are relevant. The simultaneous calibration of roughness and diameter reduction would strongly increase the number of unknowns.

To estimate the roughness coefficient of each pipeline in the network, the P_N method applied to stationary states was used together with an optimization algorithm that minimized an objective function. Three different objective functions were compared based on different hydraulic assumptions. The multi-variable problem of finding the optimum value for all the pipelines in the network and for each different steady configuration would require unmanageable experimental and computational resources. Therefore, three different cluster scenarios were designed including 3, 5 and 11 zones.

Kumar et al. (2010) proposed a practical methodology for large networks based on a clustering algorithm for automatically grouping the pipes having similar roughness characteristics into one zone. The principles of this method were applied in this research. The uncertainty about the location and level of infestation of the different pipes was overcome by the analysis of different grouping scenarios for the study network.

The absolute roughness of plastic pipes seems to vary substantially according to the type of plastic or the pipe condition (Diogo and Vilela, 2014). Even if the absolute roughness was detected relatively small in some tested pipes, it appears to have an important role in the resistance law. This may be relevant, mainly for large sections and large lengths, frequently requiring precise calculations in practical applications, and/or for relatively high Reynolds numbers. The Moody diagram provides values of friction for relative roughness between 0 and 0.05. Higher values of relative roughness are expected for moderately to high-infested pipes by zebra mussel. Other applications of flows in small diameters, such as high heat flux cooling, microfluidics and biological application (Kandlikar et al., 2005) will also require high values of relative roughness. Experiments have been performed in this research to extend the roughness ranges to 0.6962. However, experiments were only performed for a DN200 mm diameter under turbulent flow. Results should be carefully upscaled for larger diameters.

Further research in this line will include more measurement points at the piping network and several seasons of data sets. The comparison between seasons will determine if the infestation pattern depends on structural (fixed) or/and on seasonal (variable) characteristics. It would also be interesting to discriminate between the effects of mussel settlement inside the pipes and the accumulation of dead and detached shells. Mussel settlement has been analyzed in this research, a process expected to induce gradual head loss increase. According to the network managers, the second process results in a sudden head drop that has not been analyzed in this study.

The proposed Normalized Pressure method requires intense data series that not always are available. Although TM/RC systems have been widely installed in modernized irrigation networks since XXI century, the data required to adequately apply the method are not easy to find. Playán et al. (2018), in a study about TM/RC systems installed in WUAs in Spain, indicated that a large majority of the TM/RC systems (85%) are regularly used to improve water and energy management, but only 25% of them exploit most of the potential capacities of the technology. The development of applications based on TM/RC technology, such as the Normalized Pressure method, will reinforce the use and success of both, the technology and the method. However, in the short term, the development of a simplified method replacing TM/RC data by more commonly available irrigation network data constitutes a key challenge to control zebra mussel infestation.

5. Conclusions

The Normalized Pressure method has been applied to a collective pressurized irrigation network. Telemetry and remote control data sets were available, and pressure recorders were installed at specific hydrants. The method permitted to characterize pipe roughness, which was associated to zebra mussel settlement. The application of the method underlined the importance of data quality. Quality data control procedures were proposed and applied to pressure data.

Different objective functions were used for the optimization process, providing similar estimations of pipe roughness. The network-zoning scenario had a major role on pipe roughness values. The division of the network into zones of similar pipe absolute roughness should be performed taking into account the existence of sufficient pressure measurement points. The optimized pipe absolute roughness values summarizes the effect of section constriction and the increase on wall shear stress. No attempt was made to separate both effects, in view of the limited availability of experimental data.

The method permitted to establish different values of pipe absolute roughness for the analyzed network zones. The values of pipe roughness were tentatively classified in six infestation levels based on laboratory experiments. The well-established hydraulic principles used in this research contribute to the validity of the results, namely of the capacity of the normalized pressure method to map zebra mussel infestation in the pipelines of a collective irrigation network. The ultimate validation of the process would require a forensic approach: extracting pipelines to verify their infestation level, a practice that is not possible in real irrigation networks.

Intensive research on this methodology (more density of observation points, several irrigation campaigns) would permit to take a decisive step in its application: decision making on management practices and chemical treatments. Observing the evolution of infestation in network zones and establishing cost efficient thresholds protecting network operability would lead to informed decision making about chemical treatments applied to the complete network or to parts of it. Continuous monitoring of normalized pressure would permit to separate the effects of mussels and those of dead shells, ideally predicting the accumulation of shells following a chemical treatment.

6. Acknowledgements

Thanks are due to the managers of the Almudévar Water Users Associations, Felipe, Javier and Nati. Their cooperation made this research possible.

Funding: This work was supported by the State Research Agency of the Government of Spain (Agencia Estatal de Investigación) through grant AGL2017-89407-R and by the European Agricultural Fund for Rural Development (EAFRD) and the Government of Aragón. Both institutions funded the IRRIZEB II (*Programa integral para el control y mitigación del impacto de la plaga de Mejillón Cebra en sistemas de regadío II*) grant of the *Plan de Desarrollo Rural* (PDR).

7. References

Abdulshaheed, A., Mustapha, F., Ghavamian, A. 2017. A pressure-based method for monitoring leaks in a pipe distribution system: A Review. Renewable and Sustainable Energy Reviews 69: 902-911.

Aldridge, D.C., Elliott, P. Moggridge, G.D. 2004. The recent and rapid spread of the zebra mussel (Dreissena polymorpha) in Great Britain. Biological Conservation, 119(2): 253-261.

Araujo R. 2006. La afección del mejillón cebra y su posible lucha en las infraestructuras, especialmente en los riegos tradicionales y modernizados del Levante Ibérico. Unpublished report, 42 pp. [in Spanish]. https://www.chj.es/ (accessed Decem, 2020).

Benson, A.J., Raikow, D., Larson, J., Fusaro, A., Bogdanoff, A.K., and Elgin, A., 2021, Dreissena polymorpha (Pallas, 1771): U.S. Geological Survey, Nonindigenous Aquatic Species Database, Gainesville, FL, https://nas.er.usgs.gov/queries/FactSheet.aspx?speciesID=5, Revision Date: 5/17/2021, Access Date: 9/21/2021.

Bezerra A.A., Castro, M.A.H. and de Andrade Araújo R.S. 2017. Absolute roughness calculation by the friction factor calibration using the Alternative Hydraulic Gradient Iterative Method on water distribution networks. Brazilian Journal of Water Resources vol. 22.

Boxall, J. B., Saul, A. J., and Skipworth, P. J. 2004. Modeling for hydraulic capacity. J. AWWA, 96(4), 161-169.

Catita, D., Gama, M., Azedo, R., Banha, F., Pinto, J., Ilheu, A. and Anastacio, P. 2020. Detection and possible elimination of the first recorded population of the zebra mussel (Dreissena polymorpha) in Portugal from a reservoir. Management of biological invasions, 11(3), 406-414.

Chaparro, B., Thuillier, S., Menezes, L., Manach, P., and Fernandes,J. 2008. Material parameters identification: Gradient-based, genetic and hybrid optimization algorithms. Comp. Math. Sci., 44(2), 339 – 346.

CHE. 2018. Control larvario de especies exóticas invasoras en las masas de agua superficiales (embalses) de la cuenca del Ebro. Campaña 2018, 135 pp. (available at http://www.chebro.es).

Christensen, R.T. and Barfuss, S.L. 2009. Improving water quality modeling in systems containing tuberculated pipes Proc., Annual Conference and Exposition 2009, AWWA, San Diego, CA.

Clark, R.M. and Haught, C.H. 2005. Characterizing pipe wall demand: Implications for water quality modeling. J. Water Resour. Plan. Manage., 131(3), 208-217.

de Schaetzen, W.B.F., Walters, G.A., and Savic, D.A., 2000. Optimal sampling design for model calibration using shortest path, genetic and entropy algorithms. Urban Water 2: 141-152

Diogo, A.F and Vilela, F.A. 2014. Head losses and friction factors of steady turbulent flows in plastic pipes. Urban Water Journal, 11:5, 414-425, DOI: 10.1080/1573062X.2013.768682

Hallam, N.B., West, J.R., Forster, C.F., Powell, J.C., and Spencer, I. 2002.The decay of chlorine associated with the pipe wall in water distribution systems. Water Res., 36(14), 3479-3488.

Johnson, S.G. 2017. The NLopt nonlinear-optimization package, http://github.com/stevengj/nlopt

Kandlikar, S.G., Schmitt, D., Carrano, A.L., Taylor, J.B. 2005. Characterization of Surface Roughness Effect on Pressure Drop in Single-Phase Flow in Minichannels. Physics of Fluids 17, 100606.

Kumar, S.M., Narasimhan, S., Bhallamudi, S.M. 2010. Parameter Estimation in Water Distribution Networks. Water Resour Manage 24:1251–1272

Morales-Hernández, M., Playán, E., Gimeno, Y., Serreta, A. and Zapata, N. 2018. Assessing zebra mussel colonization of collective pressurized irrigation networks through pressure measurements and simulations. Agric. Wat. Manage. 204: 301-313.

Morales, J., Lizana, M., Flechoso, F., Bejarano, G.M. and Negro, A.I. 2019. Estimate zebra mussel veliger density from the riverbanks, lotic stretch and reservoir, in two Mediterranean rivers (E Spain). Knowl. Manag. Aquat. Ecosyst. 420, 7. https://doi.org/10.1051/kmae/2018042.

Moody, L.F. 1944. Friction Factors for Pipe Flow. Transactions of the American Society of Mechanical Engineers, 66, 671-681.

Mugunthan, P., Shoemaker, C.A., Regis, R.G. 2005. Comparison of function approximation, heuristic, andderivative-based methods for automatic calibration of computationally expensive groundwater bioreme-diation models. Water Resour. Res.41, W11427.

Nakano, D., Strayer, D.L. 2014. Biofouling animals in fresh water: biology, impacts, and ecosystem engineering. Front Ecol Environ 12:167–175

Olson, J, Robertson, J.J., Swannack, T.M., McMahon, R.F., Nowlin, W.H., and Schwalb, A.N. 2018. Dispersal of zebra mussels (Dreissena polymorpha) downstream of an invaded reservoir. Aquatic Invasions 13(2): 199–209. DOI: https://doi.org/10.3391/ai.2018.13.2.02

Paterson Earth & Water Consulting. 2018. Dreissenid Mussels and Alberta's Irrigation Infrastructure: Strategic Pest Management Plan and Cost Estimate. Prepared for the Eastern Irrigation District, Brooks, Alberta. 130 pp.

Pérez, R., Puig, V., Pascual, J., Quevedo, J., Landeros, E., Peralta, A. 2011. Methodology for leakage isolation using pressure sensitivity analysis in water distribution networks. Control Eng. Pract. 19(10):1157–67.

Playán, E., Salvador, R, Bonet, L., Camacho, E., Intrigliolo, D., Moreno, M.A., Rodriguez-Díaz, J.A., Tarjuelo, J.M., Madurga, C., Zazo, T., Sánchez-de-Ribera, A., Cervantes, A. and Zapata N. 2018. Assessing Telemetry and Remote Control Systems for Water Users Associations in Spain. Agric. Wat. Manage. 202: 89-98.

Powell, M. J. D. 2009. The BOBYQA algorithm for bound constrained optimization without derivatives," Department of Applied Mathematics and Theoretical Physics, Cambridge England, technical report NA2009/06..

Roberts, L. 1990. Zebra Mussel Invasion Threatens U.S. Waters. Science, New Series, 249(4975):1370-1372.

Rossman, L.A. 2000. EPANET 2 User´s Manual. US Environ. Prot. Agency, Washington, D.C. EPA/600/R-00/057.

Taylor, J.B., Carrano, A.L. and Kandlikar, S.G. 2006. Characterization of the effect of surface roughness and texture on fluid flow - past, present and future. International Journal of Thermal Science 45: 962-968.

Waller, D.L., Fisher, S.W. 1998. Evaluation of several chemical disinfectants for removing zebra mussels from unionid mussels. Progressive Fish-Culturist, 60(4):307-310.

Walski, T. M. 2000. Model calibration data: the good, the bad and the useless. J. AWWA, 92(1), 94-99.

Walski, T. M. 2004. Discussion: Modeling for hydraulic capacity. J. AWWA, 96(10), 104-108.

Wimbush, J., M. E. Frischer, J. W. Zarzynski, and S. A. Nierzwicki-Bauer. 2009. Eradication of colonizing populations of Zebra Mussels (Dreissena polymorpha) by early detection and SCUBA removal: Lake George, NY. Aquatic Conservation: Marine and Freshwater Ecosystems 19:703–713.

Zhang Ch, Xua, M., Wang, Z., Liu, W., Yub, D. 2017. Experimental study on the effect of turbulence in pipelines on the mortality of Limnoperna fortunei veligers. Ecological Engineering 109:101–118.

Table 1. Sensitivity analysis for the 3-zone scenario. Range of roughness values for each network zone.

Network zone	Absolute roughness (mm)

	Baseline	Lower limit	Upper limit	Step size
Zone 1	0.69	0.01	50	0.01
Zone 2	26.71	0.01	50	0.01
Zone 3	0.37	0.01	1	0.001

Table 2. Experimental conditions evaluated at the laboratory in a PVC pipe of DN 200 mm and 16 atmospheres.

Discharge (l s^{-1})		Half number of screws	Total number of screws
δ_{XL} * δ_{XD} (mm^2)		104.8 * 59.8	52.4 * 29.9
δ_{XH} (mm)	0	68	
	0	110	
	0	196	
	0	251	
	0	312	
δ_{XH} (mm)	20	58	-
	20	112	-
	20	193	-
	20	280	-
	20	384	-
δ_{XH} (mm)	30	58	28
	30	111	69
	30	194	139
	30	279	208
	30	377	279
δ_{XH} (mm)	40	42	17
	40	110	59
	40	195	112
	40	279	153
	40	346	193

Table 3. Intercept values at the different hydrants, □$_i$□□for the quasi-hydrostatic and the quadratic regression optimization methods.

	Intercept δ_i (kPa)

Hydrant number	Quasi-hydrostatic	Quadratic regression
H226	12.2	13.1
H234	27.0	25.6
H241	17.3	18.8
H243	12.3	13.7
H249	51.8	51.8
H256	24.0	24.3
H260	19.4	18.4
H261	42.4	40.9
H264	19.2	20.7
H275	8.8	8.4

Table 4. Computational time and number of iterations of each optimization and zoning scenario.

	3-zone	5-zone	11-zone

Optimizing method	Time (s)	Iter.	Time (s)	Iter.	Time (s)	Iter.
Quasi-hydraulic	22.1	241	45.9	500	119.0	1.301
Quadratic-regression	26.9	290	59.1	639	133.4	1.442
Null-slope	19.0	206	46.9	507	267.6	2.880

Agricultural Water Management 260: 107300 (2022)

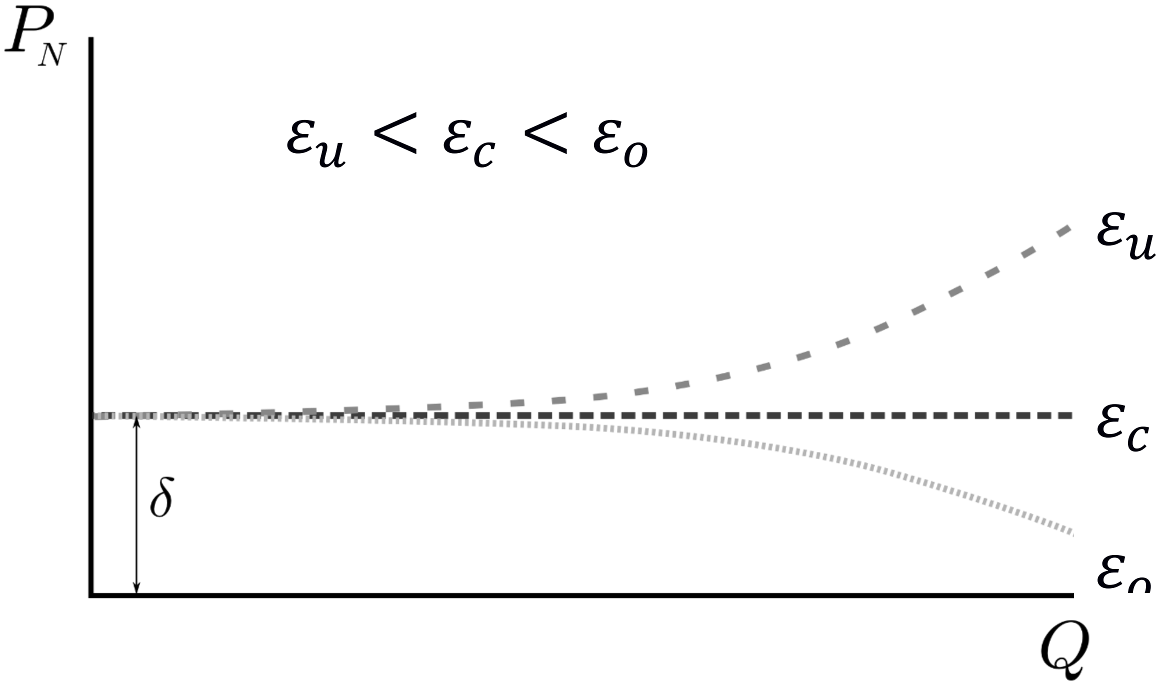

Figure 1. Normalized pressure as a function of discharge for different estimations of roughness coefficient.

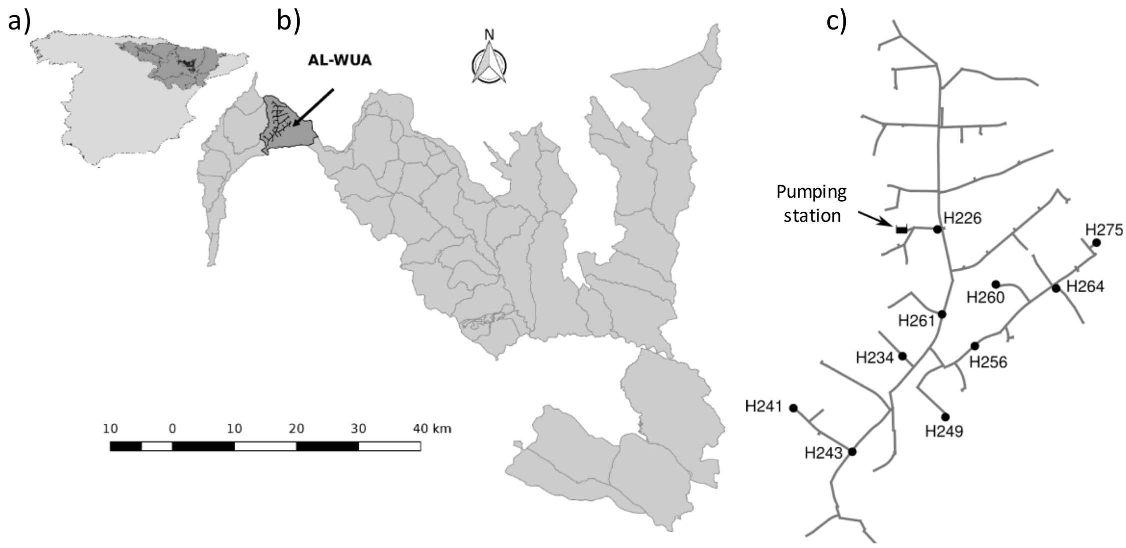

Figure 2. Location of the Ebro river basin, its provinces and the RAA project (in black) in the Iberian Peninsula (a). Map of the RAA project and its Water User Associations, highlighting the Almudévar WUA (AL-WUA) and the location of La Violada network (b). The layout of La Violada piping network locating the monitored hydrants for pressure measurements (c)

a)

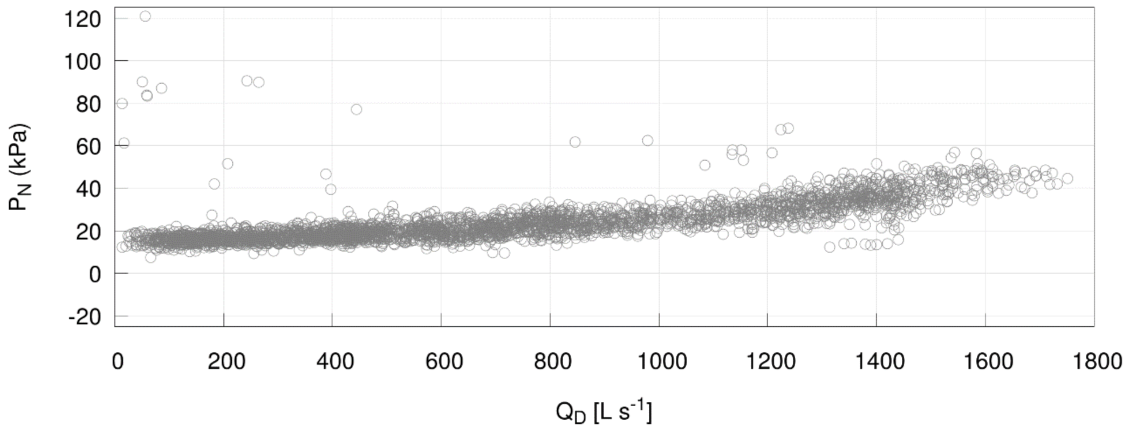

b)

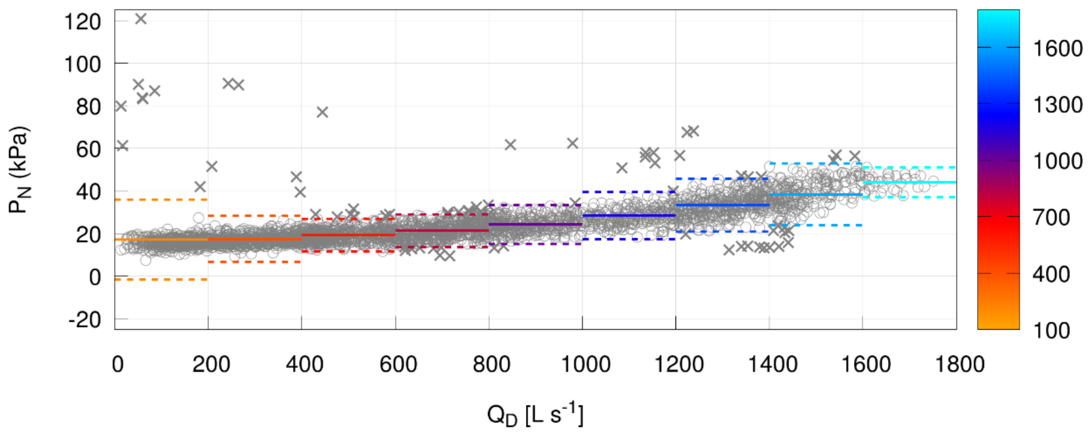

Figure 3. (a) Evolution of normalized pressure, P_N (kPa) as a function of total discharge Q_D (L s^{-1}). (b) Method used to identify outliers by discretizing Q_D in ranges of 200 L s^{-1}. Points out of the interval mean P_N (continuous segments) plus/minus two standard deviations (dashed segments) were considered outliers (crosses).

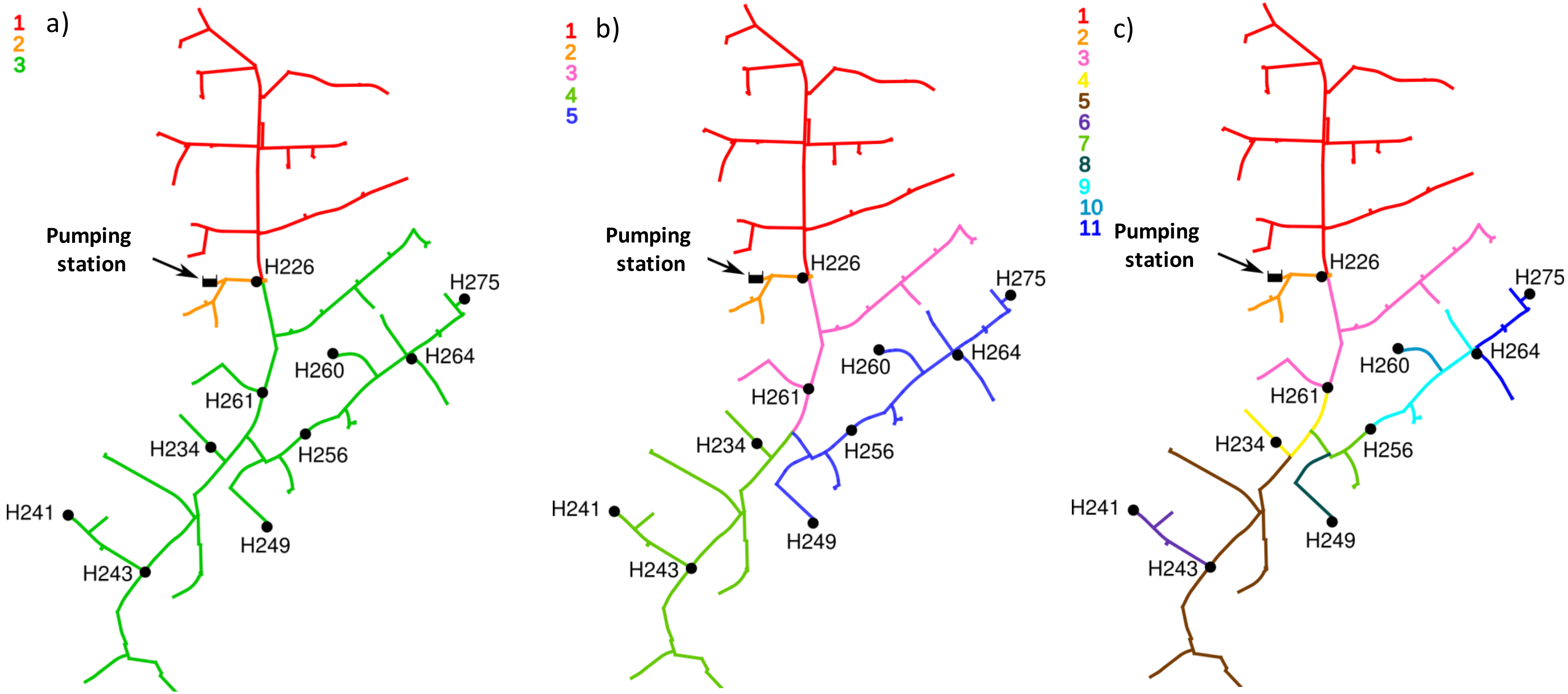

Figure 4. Network zones of the three scenarios. (a) 3-zone; (b) 5-zone; and (c) 11-zone.

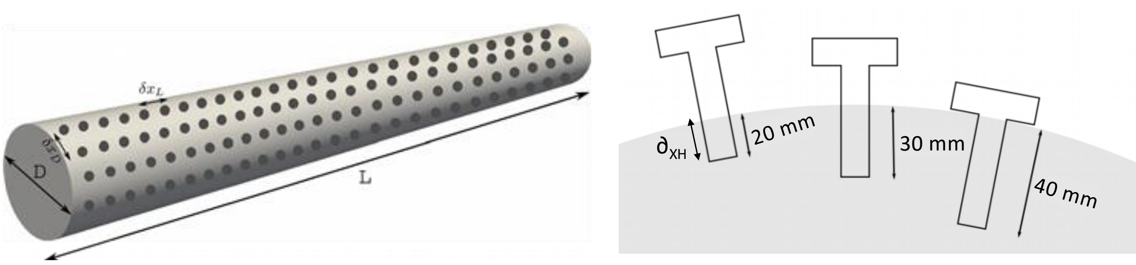

Figure 5. Longitudinal profile (a) and cross-sectional area of the experimental pipe (b).

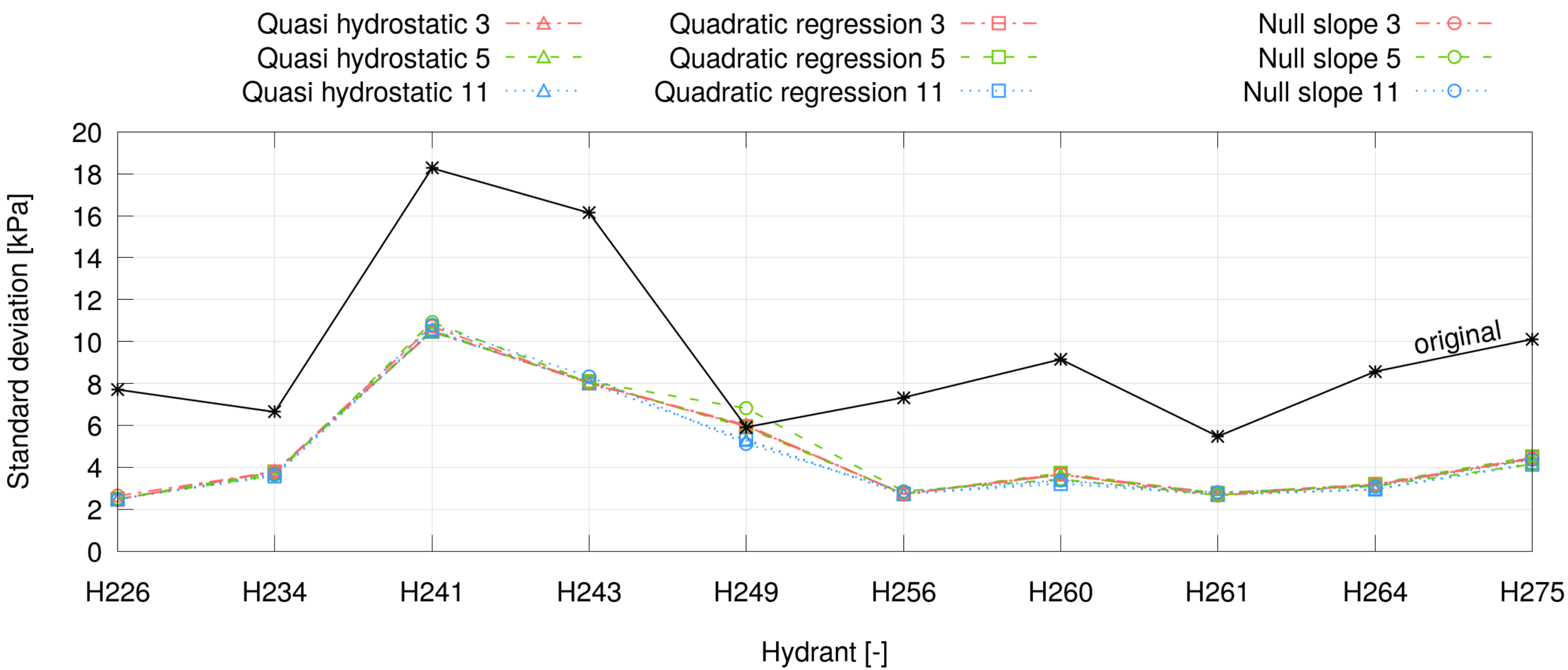

Figure 6. Standard deviation of P_N, kPa, for each optimization method and sectoring scenario at each monitored hydrant.

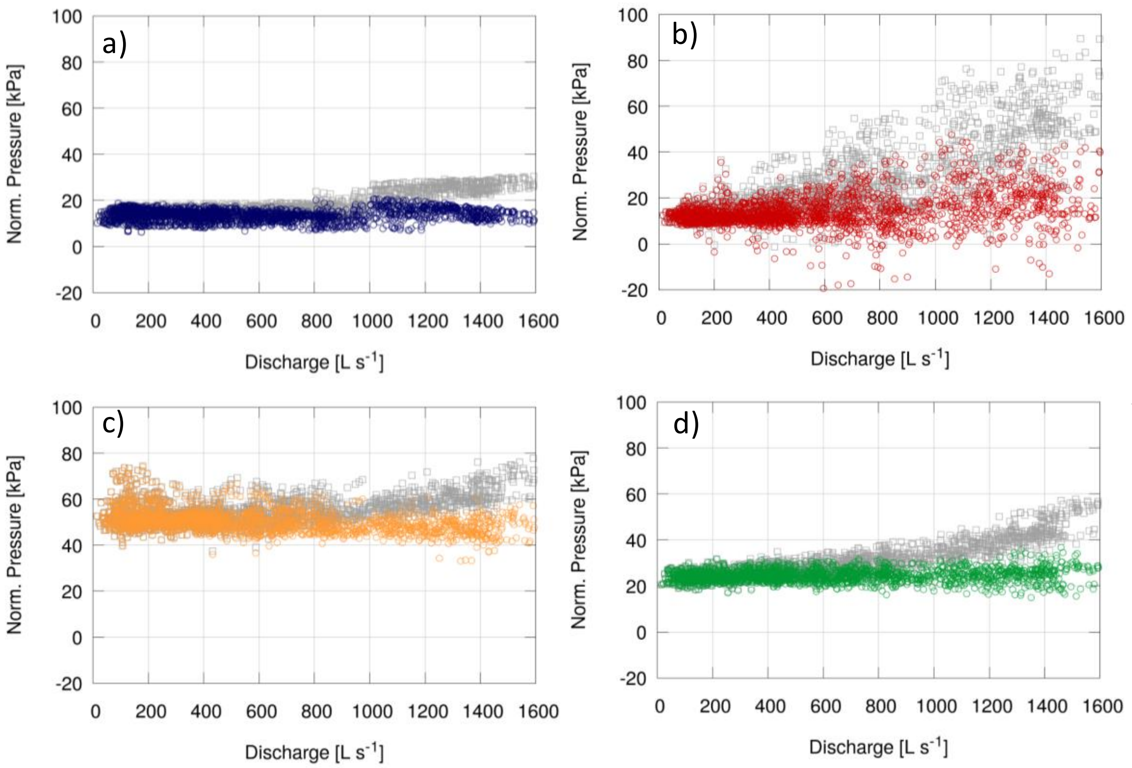

Figure 7. Original (gray square symbols) and optimized (colored circle symbols) Normalized Pressure obtained by the most efficient method at each hydrant. From left to right, upper to lower, a) H226 Quadratic regression and 3-zone; b) H243 Quadratic regression and 3-zone; c) H249 Null slope and 11-zone; and d) H256 Quasi hydrostatic and 11-zone.

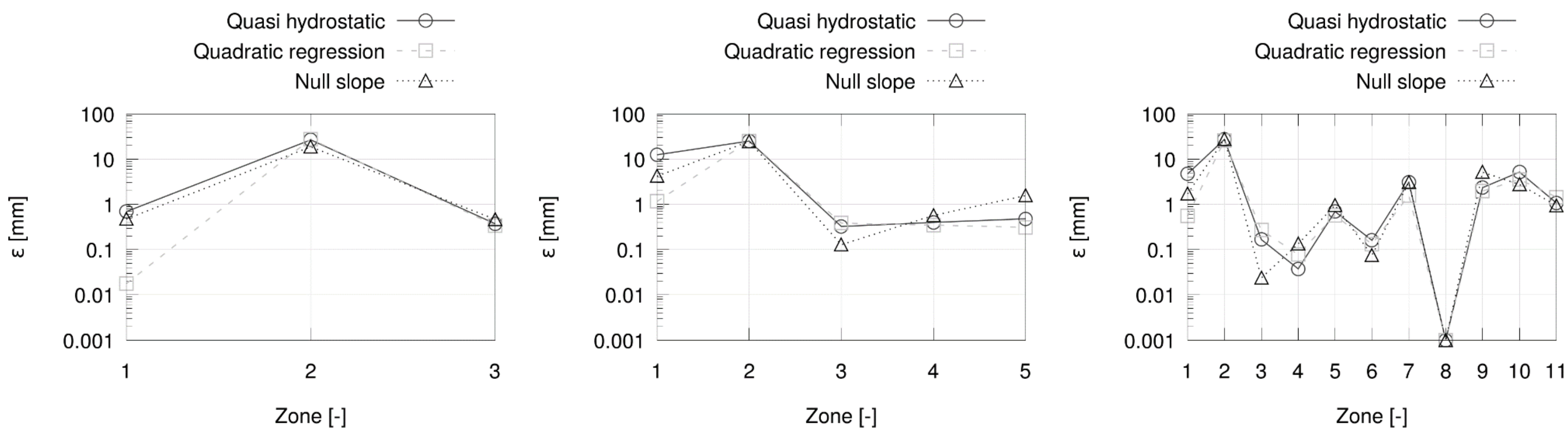

Figure 8. Values of absolute roughness (mm) for each zoning scenario (a, b and c for 3-zone, 5-zone and 11-zone scenarios) and optimization method (quasi hydrostatic, quadratic regression and null slope).

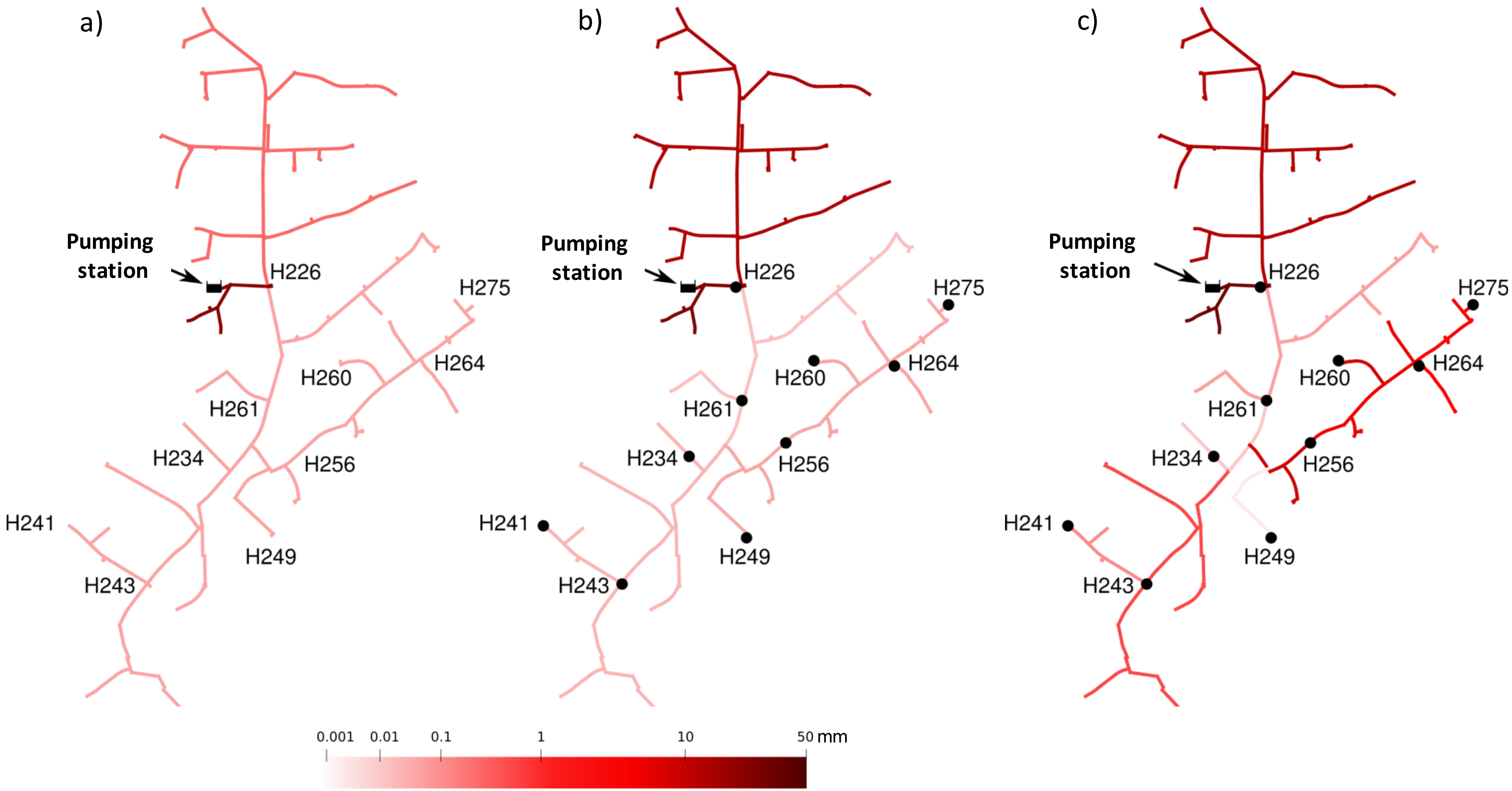

1121

1122 **Figure 9.** Maps of pipe absolute roughness for the quasi-hydrostatic optimization method and for the three zoning scenarios: (a) 3-zone, (b) 5-

1123 zone and (c) 11-zone.

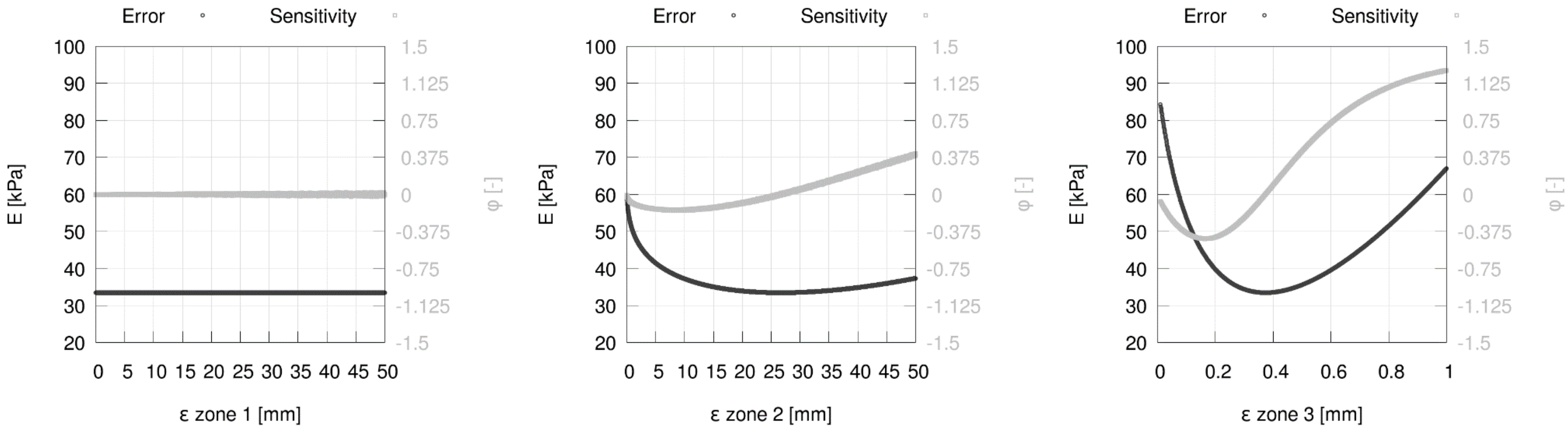

Figure 10. Error and sensitivity of absolute roughness at zones 1 (a), 2 (b) and 3 (c) for the Quasi hydrostatic 3-zone scenario.

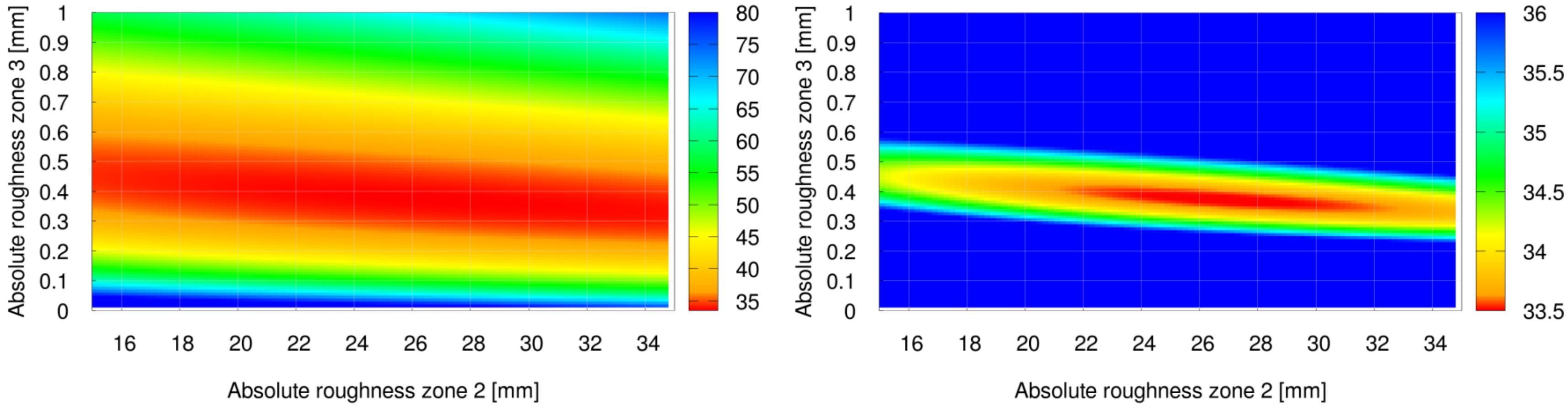

Figure 11. a) Error of the absolute roughness coefficient at zones 2 and 3 for the quasi-hydrostatic optimization method of the 3-zone scenario. b) Zoom to the values of lowest error.

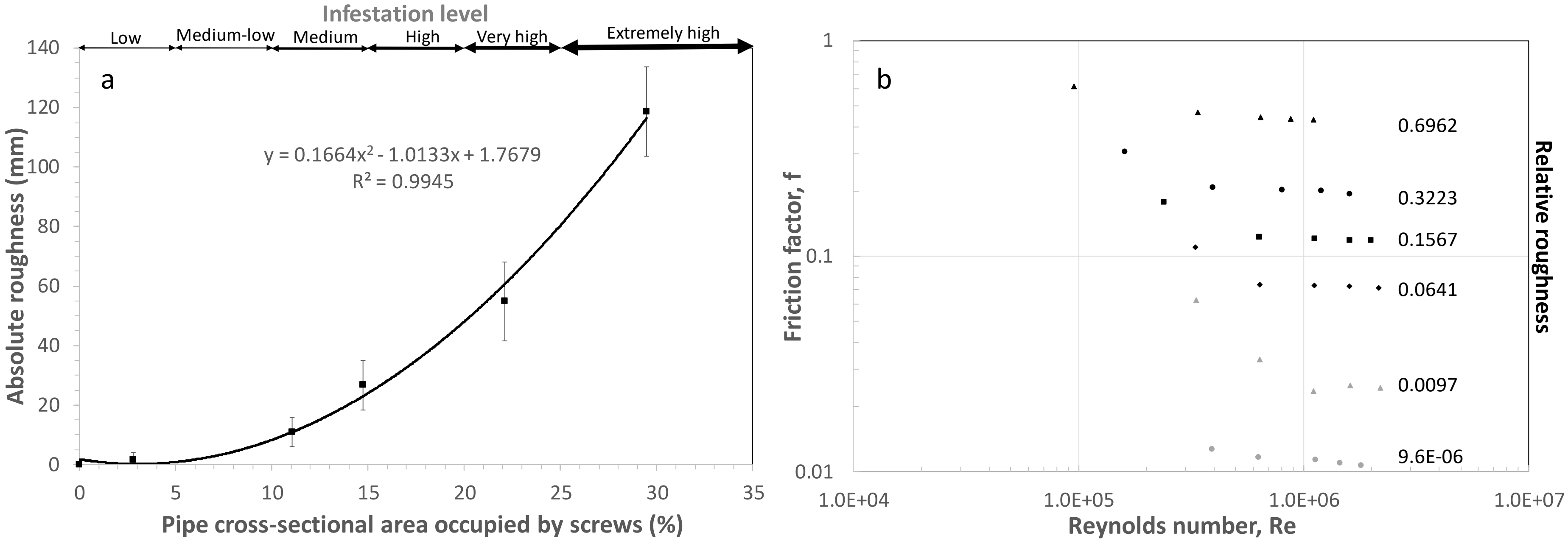

Figure 12. a) Absolute roughness values (mm) as a function of cross-sectional area occupied by zebra mussel (screws) experimentally obtained at the laboratory for a PVC pipe of DN200. Error bars represents ± one standard deviation of the average value for the five discharges evaluated at each pipe condition. The infestation level also is included in the figure as derived from ranges of cross-sectional area occupied by screws. b) Pairs of values (Re, f) measured for the PVC pipe under different values of relative roughness.